

See discussions, stats, and author profiles for this publication at: <https://www.researchgate.net/publication/257014714>

On harmonic and biharmonic Bézier surfaces

Article in *Computer Aided Geometric Design* · September 2004

DOI: 10.1016/j.cagd.2004.07.003

CITATIONS

66

READS

556

2 authors, including:



Hassan Ugail

University of Bradford

189 PUBLICATIONS 1,282 CITATIONS

SEE PROFILE

Some of the authors of this publication are also working on these related projects:



Face Recognition [View project](#)



MotiVar: Motivating weight loss through a personalised avatar [View project](#)



ELSEVIER

Available online at www.sciencedirect.com

Computer Aided Geometric Design ●●● (●●●●) ●●●—●●●

COMPUTER
AIDED
GEOMETRIC
DESIGNwww.elsevier.com/locate/cagd

On harmonic and biharmonic Bézier surfaces [☆]

J. Monterde ^{a,*}, H. Ugail ^b

^a *Departamento de Geometria i Topologia, Universitat de València, Avd. Vicent Andrés Estellés, 1, E-46100-Burjassot, València, Spain*

^b *Department of Electronic Imaging and Media Communications, School of Informatics, University of Bradford, Bradford BD7 1DP, United Kingdom*

Received 27 February 2004; received in revised form 29 June 2004; accepted 11 July 2004

Abstract

We present a new method of surface generation from prescribed boundaries based on the elliptic partial differential operators. In particular, we focus on the study of the so-called harmonic and biharmonic Bézier surfaces. The main result we report here is that any biharmonic Bézier surface is fully determined by the boundary control points. We compare the new method, by way of practical examples, with some related methods such as surfaces generation using discretisation masks and functional minimisations.

© 2004 Elsevier B.V. All rights reserved.

Keywords: Bilaplacian operator; Biharmonic surfaces; PDE freeform surfaces

1. Introduction

Given a parametric surface patch $\vec{x}: [u, v] \rightarrow \mathbb{R}^3$, the conditions that the surface to be harmonic and biharmonic respectively are given as, $\Delta \vec{x} = 0$ and $\Delta^2 \vec{x} = 0$, where $\Delta = (\frac{\partial^2}{\partial u^2} + \frac{\partial^2}{\partial v^2})$. It is well known that both the harmonic and biharmonic operators are widely used in many application areas. For example, the harmonic operator, otherwise known as the Laplacian, is associated with a wide range of physical

[☆] This work has been partially supported by a Spanish MCyT grant BFM2002-00770.

* Corresponding author.

E-mail addresses: monterde@uv.es (J. Monterde), h.ugail@bradford.ac.uk (H. Ugail).

problems such as gravity, electromagnetism and fluid flows. Similarly the biharmonic is also associated with a variety of physical problems such as tension in elastic membranes and the study of stress and strain in physical structures.

From a geometric design point of view these operators have found their way into various application areas such as surface design, geometric mesh smoothing and fairing. To this end it is noteworthy to refer to Bloor and Wilson's PDE method (Bloor and Wilson, 1990; Ugail et al., 1999; Ugail, 2003), for intuitive shape generation, based on the solution of the biharmonic PDE with appropriately chosen boundary conditions. We also take note of the work by Schneider and Kobbelt and others on geometric mesh fairing (e.g., (Schneider and Kobbelt, 2001; Kim and Rossignac, 2004; Schneider et al., 2001)), where the properties of the bi-Laplacian operator are used to fair triangular meshes.

In this paper we present a class of Bézier surfaces that are based on the elliptic operators mentioned above. Thus, here we introduce the so-called harmonic and biharmonic Bézier surfaces and we study the characterisations of such surfaces.

Harmonic surfaces are related to minimal surfaces, i.e., surfaces that minimise the area among all surfaces with prescribed boundary conditions. The relation is as follows. Given a parametric surface patch $\vec{x}(u, v)$ satisfying the isothermal conditions, i.e., $\langle \vec{x}_u, \vec{x}_u \rangle = \langle \vec{x}_v, \vec{x}_v \rangle$ and $\langle \vec{x}_u, \vec{x}_v \rangle = 0$, where \vec{x}_u, \vec{x}_v are the first derivatives of $\vec{x}(u, v)$ with respect to u and v respectively and $\langle \cdot, \cdot \rangle$ defines the dot product of the vectors, then the surface it represents is minimal if and only if it is harmonic. The main result from the theory of minimal surfaces states that, under certain conditions, given the boundary there is a unique minimal surface prescribed by that boundary.

The somewhat surprising result is that, similar to the minimal surfaces, the knowledge of the boundary of a biharmonic Bézier surface enables one to fully determine the entire surface. We compare this with the corresponding result for harmonic Bézier surfaces where the knowledge of two opposite boundary curves of the harmonic Bézier surface fully determines the surface. Naturally one would expect that biharmonic surfaces unconstrained to be a polynomial defined not only by the boundaries but also by the boundary cross-slopes. As one of the referees has rightly pointed out, somehow the 'polynomiality' determines the cross-slopes.

Our motivation for this work include the following. The use of both harmonic and biharmonic Bézier surfaces would enable surfaces to be generated and controlled using boundary curves, rather than a set of control points, where the interior of the corresponding Bézier surface can be controlled by the harmonicity conditions. Due to the harmonicity conditions one could also expect both the harmonic and biharmonic Bézier surfaces to be smooth and fair surfaces as verified later in this paper. Furthermore, the techniques we utilise to generate the harmonic and biharmonic Bézier surfaces can be adopted to approximate solutions to mathematical boundary-value problems in particular solutions to elliptic PDEs, again as indicated later in the paper.

In the rest of this section we discuss some characteristics and properties of the harmonic and biharmonic operators which form the basis for our detailed analysis of the harmonic Bézier surfaces discussed in Section 2 and the biharmonic Bézier surfaces discussed in Section 3. In Section 4 we discuss a comparative study between harmonic and biharmonic Bézier surfaces by means of numerically comparing the related functionals and extremals of the surfaces. We also make qualitative comparisons between the surfaces by means of comparing the curvature distributions on the surfaces. We undertake this comparative study using several examples.

1.1. *The associated functionals and their extremals*

We shall study some second order functionals defined on the space of smooth patches $\vec{x}: R \rightarrow \mathbb{R}^3$ where $R = [0, 1] \times [0, 1]$. Given a Lagrangian

$$L(\vec{x}) = L(\vec{x}, \vec{x}_u, \vec{x}_v, \vec{x}_{uu}, \vec{x}_{uv}, \vec{x}_{vv}),$$

we take the functional I to be such that,

$$I(\vec{x}) = \int_R L(\vec{x}) \, du \, dv. \tag{1}$$

Minimising the functional I is equivalent to requiring that the first variation of I is zero which then gives rise to the corresponding Euler–Lagrange equations. For instance, the Lagrange functional generating the Laplacian operator is

$$D(\vec{x}) = \frac{1}{2} \int_R (\|\vec{x}_u\|^2 + \|\vec{x}_v\|^2) \, du \, dv, \tag{2}$$

which is also known as the Dirichlet functional in the theory of minimal surfaces.

In a similar fashion to the harmonic functional, the Lagrange functional defining the biharmonic Laplacian operator, which we shall refer as the biharmonic functional, is

$$B(\vec{x}) = \frac{1}{2} \int_R (\|\vec{x}_{uu}\|^2 + 2\|\vec{x}_{uv}\|^2 + \|\vec{x}_{vv}\|^2) \, du \, dv. \tag{3}$$

1.2. *Finite difference discretisation and masks*

Let us assume that we are applying the harmonic operator $\Delta \vec{x} = 0$ to a given function $\vec{x}: [u, v] \rightarrow \mathbb{R}^3$. We could discretely represent this by denoting a node in the square finite difference mesh by the integers i, j , with mesh spacing h so that the coordinates $u = ih$ and $v = jh$, is in the form,

$$\frac{\vec{x}_{i+1,j} - 2\vec{x}_{i,j} + \vec{x}_{i-1,j}}{h^2} + \frac{\vec{x}_{i,j+1} - 2\vec{x}_{i,j} + \vec{x}_{i,j-1}}{h^2}. \tag{4}$$

Rearranging Eq. (4) gives us an expression of the form,

$$\vec{x}_{i,j} = \frac{1}{4} [\vec{x}_{i+1,j} + \vec{x}_{i-1,j} + \vec{x}_{i,j+1} + \vec{x}_{i,j-1}]. \tag{5}$$

The statement in Eq. (5) can be diagrammatically represented in the form of the following harmonic mask,

$$\frac{1}{4} \begin{matrix} 0 & 1 & 0 \\ 1 & \bullet & 1 \\ 0 & 1 & 0 \end{matrix} \tag{6}$$

Here the mask is considered to be a stencil for the central point. Similar masks have been used by Farin and Hansford in their study of discrete Coons patches (Farin and Hansford, 1999) which can also be formulated as solutions to a suitably chosen PDE.

For the biharmonic case, the discretisation process applied to the biharmonic operator produces a kind of mask of higher order that is given as,

$$\frac{1}{20} \begin{pmatrix} 0 & 0 & 1 & 0 & 0 \\ 0 & 2 & -8 & 2 & 0 \\ 1 & -8 & \bullet & -8 & 1 \\ 0 & 2 & -8 & 2 & 0 \\ 0 & 0 & 1 & 0 & 0 \end{pmatrix} \quad (7)$$

2. Harmonic Bézier surfaces

The Euler–Lagrange equations defined by the functional in Eq. (2) are given by the harmonic equations $\Delta \vec{x} = 0$. Taking $\vec{x}: [0, 1] \times [0, 1] \rightarrow \mathbb{R}^3$ to be a Bézier surface, we seek the conditions that the function \vec{x} must fulfill in order for it to be harmonic. To this end we compute the Laplacian of the Bézier chart. The following results (Theorem 1 and Proposition 1) were obtained in (Monterde, 2003). They are included here without proof for the sake of completeness and in order to compare the results later with the corresponding results for the biharmonic case.

Theorem 1. *Given a control net in \mathbb{R}^3 , $\{P_{ij}\}_{i,j=0}^{n,m}$, the associated Bézier surface, $\vec{x}: [0, 1] \times [0, 1] \rightarrow \mathbb{R}^3$, is harmonic, i.e., $\Delta \vec{x} = 0$, if and only if for any $i \in \{1, \dots, n\}$ and $j \in \{1, \dots, m\}$*

$$\begin{aligned} 0 = & P_{i+2,j}a_{n,i,0} + P_{i+1,j}(a_{n,i-1,1} - 2a_{n,i,0}) \\ & + P_{i-1,j}(a_{n,i-1,1} - 2a_{n,i-2,2}) + P_{i-2,j}a_{n,i-2,2} \\ & + P_{i,j+2}a_{m,j,0} + P_{i,j+1}(a_{m,j-1,1} - 2a_{m,j,0}) \\ & + P_{i,j-1}(a_{m,j-1,1} - 2a_{m,j-2,2}) + P_{i,j-2}a_{m,j-2,2} \\ & + P_{ij}(a_{n,i,0} - 2a_{n,i-1,1} + a_{n,i-2,2} \\ & + a_{m,j,0} - 2a_{m,j-1,1} + a_{m,j-2,2}), \end{aligned}$$

where, for $i \in \{0, \dots, n-2\}$

$$a_{ni0} = (n-i)(n-i-1), \quad a_{ni1} = 2(i+1)(n-i-1), \quad a_{ni2} = (i+1)(i+2),$$

and $a_{nik} = 0$ otherwise, and with the convention $P_{ij} = 0$ if $i \notin \{0, \dots, n\}$ or $j \notin \{0, \dots, m\}$.

Here we can state that the harmonic condition implies that some of the control points can be expressed as linear combinations of the other control points, i.e., the first and last rows of control points fully determine the harmonic Bézier surface. Its proof can found in (Monterde, 2003).

Proposition 1. *Let $\vec{x}(u, v) = \sum_{k,\ell=0}^n B_k^n(u)B_\ell^n(v)P_{k\ell}$ be a harmonic Bézier chart of degree n with control net $\{P_{k\ell}\}_{k,\ell=0}^n$, then*

- (1) *If n is odd, control points in the inner rows $\{P_{k\ell}\}_{k=1,\ell=0}^{n-1,n}$ are determined by the control points in the first and last rows, $\{P_{0\ell}\}_{\ell=0}^n$ and $\{P_{n\ell}\}_{\ell=0}^n$.*

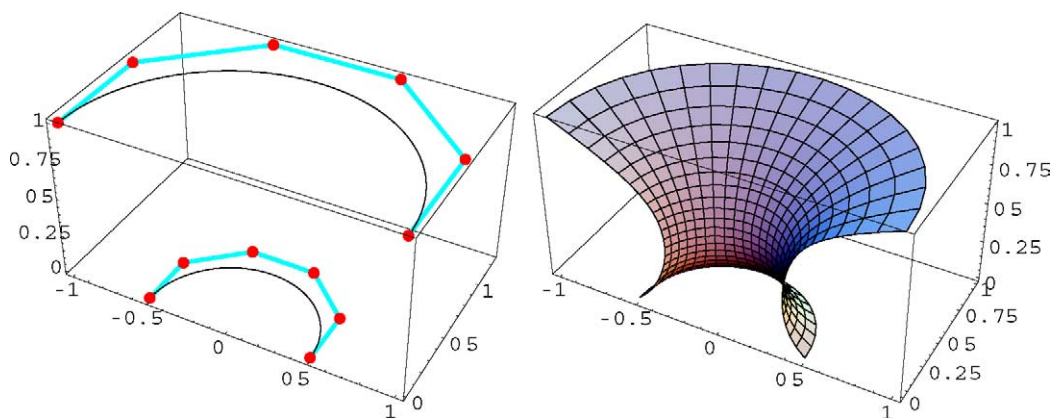


Fig. 1. Left: Boundary curves for the model problem, defined as semi-circular arcs of radius 1 and 0.5. Right: The associated harmonic Bézier surface corresponding to the boundary curves shown on the left.

(2) If n is even, control points in the inner rows $\{P_{k\ell}\}_{k=1,\ell=0}^{n-1,n}$ and also the corner control points P_{nn} are determined by the control points in the first and last rows, $\{P_{0\ell}\}_{\ell=0}^n$ and $\{P_{n\ell}\}_{\ell=0}^{n-1}$.

2.1. Model problem

In order to be able to carry out our analysis and compare different methods we have chosen to utilise an example model problem. The problem is essentially that of generating the blending surface between two semi-circular arcs of different radii as shown in Fig. 1. The boundary curves in this case are defined as Bézier curves defined by a control polygon. For example, a degree 5 Bézier approximation of the semicircle of radius 1 is the one defined by the control polygon,

$$\begin{aligned} &(-1, 0), \quad (-1, 0.72), \quad (-0.515308, 1.25143), \\ &(0.515308, 1.25143), \quad (1, 0.72), \quad (1, 0). \end{aligned}$$

For convenience, we shall refer to these curves as the ‘edge curves’. Furthermore, the other two border curves joining the corresponding end points of edge curves shall be referred to as ‘side curves’. The associated harmonic Bézier surface is shown in Fig. 1.

3. Biharmonic Bézier surfaces

3.1. The biharmonic condition

Following a similar fashion to the harmonic case, let us now ask for the conditions that a Bézier surface must fulfil in order to be biharmonic.

We shall need a lemma first. Let us compute how a Bernstein polynomial can be written as a linear combination of Bernstein polynomials of higher degree.

Lemma 1. Given a Bernstein polynomial $B_i^{n-k}(t)$ we have,

$$B_i^{n-k}(t) = \sum_{\ell=0}^k \frac{\binom{n-i-\ell}{k-\ell} \binom{i+\ell}{\ell}}{\binom{n}{k}} B_{i+\ell}^n(t),$$

for any $n > 0$, $k \in \{0, 1, \dots, n\}$ and $i \in \{0, 1, \dots, n - k\}$.

Theorem 2. Given a control net in \mathbb{R}^3 , $\{P_{ij}\}_{i,j=0}^{n,m}$, the associated Bézier surface, $\vec{x}: [0, 1] \times [0, 1] \rightarrow \mathbb{R}^3$, is biharmonic, i.e. $\Delta^2 \vec{x} = 0$ if and only if for any $i \in \{1, \dots, n\}$ and $j \in \{1, \dots, m\}$

$$\sum_{k=0}^4 b_{n,i-k,k} \Delta^{4,0} P_{i-k,j} + 2 \sum_{k,\ell=0}^2 a_{n,i-k,k} a_{m,j-\ell,\ell} \Delta^{2,2} P_{i-k,j-\ell} + \sum_{\ell=0}^4 b_{m,j-\ell,\ell} \Delta^{0,4} P_{i,j-\ell}, \quad (8)$$

where, for $i \in \{0, \dots, n - 2\}$

$$\begin{aligned} a_{ni0} &= (n - i)(n - i - 1), \\ a_{ni1} &= 2(i + 1)(n - i - 1), \\ a_{ni2} &= (i + 1)(i + 2), \end{aligned}$$

and $a_{nik} = 0$ otherwise, and for $i \in \{0, \dots, n - 4\}$

$$\begin{aligned} b_{ni0} &= (n - i)(n - i - 1)(n - i - 2)(n - i - 3), \\ b_{ni1} &= 4(i + 1)(n - i - 1)(n - i - 2)(n - i - 3), \\ b_{ni2} &= 6(i + 1)(i + 2)(n - i - 2)(n - i - 3), \\ b_{ni3} &= 4(i + 1)(i + 2)(i + 3)(n - i - 3), \\ b_{ni4} &= (i + 1)(i + 2)(i + 3)(i + 4), \end{aligned}$$

and $b_{nik} = 0$ otherwise.

Proof. We will compute the bilaplacian of the chart of the Bézier surface.

$$\begin{aligned} \Delta^2 \vec{x}(u, v) &= \left(\frac{\partial^2}{\partial u^2} + \frac{\partial^2}{\partial v^2} \right)^2 \vec{x}(u, v) = \left(\frac{\partial^2}{\partial u^2} + \frac{\partial^2}{\partial v^2} \right) \left(n(n-1) \sum_{i=0}^{n-2} \sum_{j=0}^m B_i^{n-2}(u) B_j^m(v) \Delta^{2,0} P_{ij} \right. \\ &\quad \left. + m(m-1) \sum_{i=0}^n \sum_{j=0}^{m-2} B_i^n(u) B_j^{m-2}(v) \Delta^{0,2} P_{ij} \right) \\ &= n(n-1)(n-2)(n-3) \sum_{i=0}^{n-3} \sum_{j=0}^m B_i^{n-4}(u) B_j^m(v) \Delta^{4,0} P_{ij} \\ &\quad + 2n(n-1)m(m-1) \sum_{i=0}^{n-2} \sum_{j=0}^{m-2} B_i^{n-2}(u) B_j^{m-2}(v) \Delta^{2,2} P_{ij} \\ &\quad + m(m-1)(m-2)(m-3) \sum_{i=0}^n \sum_{j=0}^{m-4} B_i^n(u) B_j^{m-4}(v) \Delta^{0,4} P_{ij}, \quad (9) \end{aligned}$$

where $\Delta^{4,0}$, $\Delta^{2,2}$ and $\Delta^{0,4}$ are the usual difference operators.

We shall rewrite expression (9) again as a Bézier surface of degrees n and m . In order to do this, we will need to apply the previous Lemma 1. Then we have,

$$\begin{aligned} B_i^{n-2}(t) &= \binom{n-2}{i} \sum_{k=0}^2 \frac{\binom{2}{k}}{\binom{n}{i+k}} B_{i+k}^n(t) \\ &= \frac{1}{n(n-1)} ((n-i)(n-i-1)B_i^n(t) \\ &\quad + 2(i+1)(n-i-1)B_{i+1}^n(t) + (i+1)(i+2)B_{i+2}^n(t)), \\ &= \frac{1}{n(n-1)} (a_{ni0}B_i^n(t) + a_{ni1}B_{i+1}^n(t) + a_{ni2}B_{i+2}^n(t)), \end{aligned}$$

for $i \in \{0, \dots, n-2\}$ and

$$\begin{aligned} B_i^{n-4}(t) &= \binom{n-4}{i} \sum_{k=0}^4 \frac{\binom{4}{k}}{\binom{n}{i+k}} B_{i+k}^n(t) \\ &= \frac{1}{n(n-1)(n-2)(n-3)} ((n-i)(n-i-1)(n-i-2)(n-i-3)B_i^n(t) \\ &\quad + 4(i+1)(n-i-1)(n-i-2)(n-i-3)B_{i+1}^n(t) \\ &\quad + 6(i+1)(i+2)(n-i-2)(n-i-3)B_{i+2}^n(t) \\ &\quad + 4(i+1)(i+2)(i+3)(n-i-3)B_{i+3}^n(t) \\ &\quad + (i+1)(i+2)(i+3)(i+4)B_{i+4}^n(t)) \\ &= \frac{1}{n(n-1)(n-2)(n-3)} \\ &\quad \times (b_{ni0}B_i^n(t) + b_{ni1}B_{i+1}^n(t) + b_{ni2}B_{i+2}^n(t) + b_{ni3}B_{i+3}^n(t) + b_{ni4}B_{i+4}^n(t)), \end{aligned}$$

for $i \in \{0, \dots, n-4\}$.

Therefore, $\Delta^2 \vec{x}(u, v) = \sum_{i=0}^n \sum_{j=0}^m B_i^n(u) B_j^m(v)$

$$\times \left(\sum_{k=0}^4 b_{n,i-k,k} \Delta^{4,0} P_{i-k,j} + 2 \sum_{k,\ell=0}^2 a_{n,i-k,k} a_{m,j-\ell,\ell} \Delta^{2,2} P_{i-k,j-\ell} + \sum_{\ell=0}^4 b_{m,j-\ell,\ell} \Delta^{0,4} P_{i,j-\ell} \right).$$

This expression can be seen as the Bézier surface associated with a net of control points $\{Q_{ij}\}_{i,j=0}^{n,m}$. Thus, due to the fact that $\{B_i^n(u) B_j^m(v)\}_{i,j=0}^{n,m}$ is a basis of bivariate polynomials, we get \vec{x} to be biharmonic if and only if $Q_{ij} = 0$ for all i, j . \square

Note that the first case where the biharmonic equation makes sense is for $n = m = 3$. In this case, the solution of Eq. (8) is

$$P_{11} = \frac{1}{9}(-4P_{00} + 6P_{01} - 2P_{03} + 6P_{10} + 3P_{13} - 2P_{30} + 3P_{31} - P_{33}),$$

$$P_{12} = \frac{1}{9}(-2P_{00} + 6P_{02} - 4P_{03} + 3P_{10} + 6P_{13} - P_{30} + 3P_{32} - 2P_{33}),$$

$$P_{21} = \frac{1}{9}(-2P_{00} + 3P_{01} - P_{03} + 6P_{20} + 3P_{23} - 4P_{30} + 6P_{31} - 2P_{33}),$$

$$P_{22} = \frac{1}{9}(-P_{00} + 3P_{02} - 2P_{03} + 3P_{20} + 6P_{23} - 2P_{30} + 6P_{32} - 4P_{33}).$$

3.2. Solving for the biharmonic condition

After studying some examples in low dimensions, it is possible to prove that the biharmonic condition implies that the inner control points of a biharmonic Bézier surface can be expressed as linear combinations of boundary control points.

In order to prove the general result, it is better to work with the usual basis of polynomials first instead of with the Bernstein basis.

Lemma 2. Let $f(u, v) = \sum_{k,\ell=0}^{n,m} \frac{a_{k\ell}}{k!\ell!} u^k v^\ell$ be a biharmonic polynomial function of degrees $n, m \geq 4$, then, all coefficients $\{a_{k\ell}\}_{k=4,\ell=0}^m$ are totally determined by the coefficients $\{a_{0\ell}, a_{1\ell}, a_{2\ell}, a_{3\ell}\}_{\ell=0}^m$.

Proof. The biharmonic condition $\Delta^2 f = 0$ can be translated into a system of linear equations in terms of the coefficients $\{a_{k\ell}\}_{k,\ell=0}^{n,m}$

$$a_{k+4,\ell} + 2a_{k+2,\ell+2} + a_{k,\ell+4} = 0, \quad k = 0, \dots, n, \ell = 0, \dots, m, \tag{10}$$

but with the convention $a_{k,\ell} = 0$ if $k > n$ or $\ell > m$.

This means that any coefficient $a_{k\ell}$ with $k > 3$ can be related to $a_{k-2,\ell+2}$ and $a_{k-4,\ell+4}$ and so on until the first subindex is smaller than 4, or until the second subindex is greater than m . \square

Remark 1. The result of Lemma 2 is not at all surprising. Note that the first four rows of coefficients determine one boundary curve and the first three transversal partial derivatives along it. Thus, they are a kind of initial Cauchy conditions of the fourth order differential equation $\Delta^2 f = 0$.

After having worked with some examples in low dimensions one can easily arrive at the statement of the following lemma:

Lemma 3. Let $r \geq 4$. If the coefficients $a_{r0}, a_{r-1,1}, a_{1,r-1}$ and a_{0r} are known, then the linear system defined by the equations of the kind given in Eq. (10) for $k + \ell = r$ ($r - 3$ equations) and with the unknowns $\{a_{k\ell}\}, k + \ell = r, k, \ell \geq 2$, has a unique solution.

Proof. The proof consists of a long but straightforward computation of the determinant of the matrix of coefficients of the linear system.

Let us write the first equations starting with $a_{r,0}$.

$$\begin{aligned} a_{r,0} + 2a_{r-2,2} + a_{r-4,4} &= 0, \\ a_{r-2,2} + 2a_{r-4,4} + a_{r-6,6} &= 0, \\ a_{r-4,4} + 2a_{r-6,6} + a_{r-8,8} &= 0. \\ \dots & \dots \end{aligned}$$

The associated matrix starts as follows (recall that $a_{r,0}$ is already known)

$$\begin{pmatrix} 2 & 1 & 0 & 0 & \dots \\ 1 & 2 & 1 & 0 & \dots \\ 0 & 1 & 2 & 1 & \dots \\ & & \ddots & \ddots & \ddots \end{pmatrix}$$

and its determinant is $c + 1$ if the number of rows of the matrix is c .

So, there exists a unique solution.

An analogous study can be carried out for the set of equations starting from $a_{r-1,1}$. \square

Now, let us come back to the Bézier form.

Proposition 2. Let $\vec{x}_{n,m}(u, v) = \sum_{k,\ell=0}^{n,m} B_k^n(u) B_\ell^m(v) P_{k\ell}$ be a biharmonic Bézier chart of degrees n, m with control net $\{P_{k\ell}\}_{k,\ell=0}^{n,m}$. Then all the inner control points $\{P_{k\ell}\}_{k=1,\ell=1}^{n-1,m-1}$ are determined by the boundary control points, $\{P_{0\ell}\}_{\ell=0}^m$, $\{P_{n\ell}\}_{\ell=0}^m$, $\{P_{k0}\}_{k=0}^n$ and $\{P_{kn}\}_{k=0}^n$.

Remark 2. The boundary control points are

$$\begin{matrix} P_{00} & P_{01} & P_{02} & \dots & P_{0m-1} & P_{0m} \\ P_{10} & * & * & \dots & * & P_{1m} \\ P_{20} & * & * & \dots & * & P_{2m} \\ \vdots & \vdots & \vdots & \ddots & \vdots & \vdots \\ P_{n-1,0} & * & * & \dots & * & P_{n-1,m} \\ P_{n0} & P_{n1} & P_{n2} & \dots & P_{n,m-1} & P_{nm} \end{matrix}$$

Proof. Let us write the Bézier chart in the usual basis of polynomials

$$\vec{x}(u, v) = \sum_{k,\ell=0}^{n,m} u^k v^\ell a_{k\ell},$$

with $a_{k\ell} \in \mathbb{R}^3$.

Note that the factorial terms in the statement of Lemma 2 are now included in the coefficients $a_{k\ell}$. Note also that the boundary control points determine the four boundary curves $\vec{x}(0, v)$, $\vec{x}(1, v)$, $v \in [0, 1]$, and $\vec{x}(u, 0)$, $\vec{x}(u, 1)$, $u \in [0, 1]$. The first boundary curve is

$$\vec{x}(0, v) = \sum_{\ell=0}^m v^\ell a_{0\ell} = \sum_{\ell=0}^m B_\ell^m(v) P_{0\ell}, \tag{11}$$

and the second one is

$$\vec{x}(1, v) = \sum_{\ell=0}^m v^\ell \sum_{k=0}^n a_{k\ell} = \sum_{\ell=0}^m B_\ell^m(v) P_{n\ell}. \quad (12)$$

Analogously,

$$\vec{x}(u, 0) = \sum_{k=0}^n u^k a_{k0} = \sum_{k=0}^n B_k^n(u) P_{k0}, \quad (13)$$

and the fourth one is

$$\vec{x}(u, 1) = \sum_{k=0}^n u^\ell \sum_{\ell=0}^m a_{k\ell} = \sum_{k=0}^n B_k^n(u) P_{km}. \quad (14)$$

From Eq. (11) we can obtain, from $\{P_{0\ell}\}_{\ell=0}^m$, the coefficients $a_{0\ell}$ for $\ell = 0, \dots, m$. Analogously, from Eq. (13) we can obtain, from $\{P_{k0}\}_{k=0}^n$, the coefficients a_{k0} for $k = 0, \dots, n$.

We now show how to obtain all the coefficients $a_{k\ell}$, $k = 0, \dots, n$, $\ell = 0, \dots, m$. From Eq. (14) we can obtain $\sum_{\ell=0}^m a_{k\ell}$ from the boundary control points $\{P_{kn}\}_{k=0}^n$. But, we first note that the biharmonic condition implies that, for $k = n$,

$$\sum_{\ell=0}^m a_{n\ell} = a_{n0} + a_{n1}.$$

Therefore, we can compute a_{n1} . Similar arguments can be used to compute a_{1n} from the boundary control points $\{P_{0\ell}\}_{\ell=0}^m$ and $\{P_{n\ell}\}_{\ell=0}^m$. Now, thanks to Lemma 3, we can compute all the diagonal coefficients $a_{k\ell}$ with $k + \ell = n + 1$. Note that the biharmonic condition implies that, for $k = n - 1$,

$$\sum_{\ell=0}^m a_{n-1,\ell} = a_{n-1,0} + a_{n-1,1} + a_{n-1,2}.$$

We can now compute $a_{n-1,1}$ and with similar arguments, $a_{1,n-1}$. Finally, as before, thanks to Lemma 3 we can compute all the coefficients $a_{k\ell}$ with $k + \ell = n$. Applying the same scheme of computation recursively we can obtain all the coefficients. \square

Using the above results we have generated the biharmonic Bézier surface for the boundary conditions of the model problem is shown in Fig. 2, where the figure on the left shows the boundary conditions and the figure on the right shows the biharmonic Bézier surface.

One could now compare the results obtained here for the harmonic and biharmonic Bézier surfaces through the Propositions 1 and 2, respectively. To this end we note that we are dealing with polynomial surfaces which are based on the biharmonic operator which is of order 4 and the Laplacian operator which is of order 2. Therefore, naturally the biharmonic equation $\Delta^2 \vec{x} = 0$ leaves more degrees of freedom when compared with the harmonic equation $\Delta \vec{x} = 0$.

It should be pointed that the proof of Proposition 2 offers an alternative way of solving the biharmonic equations, i.e., Eq. (8). Indeed, following the steps given along the proof one can compute the biharmonic Bézier surface defined by a configuration of the boundary control points by simply solving a system of linear equations recursively. Once the Bézier surface has been obtained, the computation of its control net is just a consequence of a change of basis. On the other hand, direct computation of the solution of

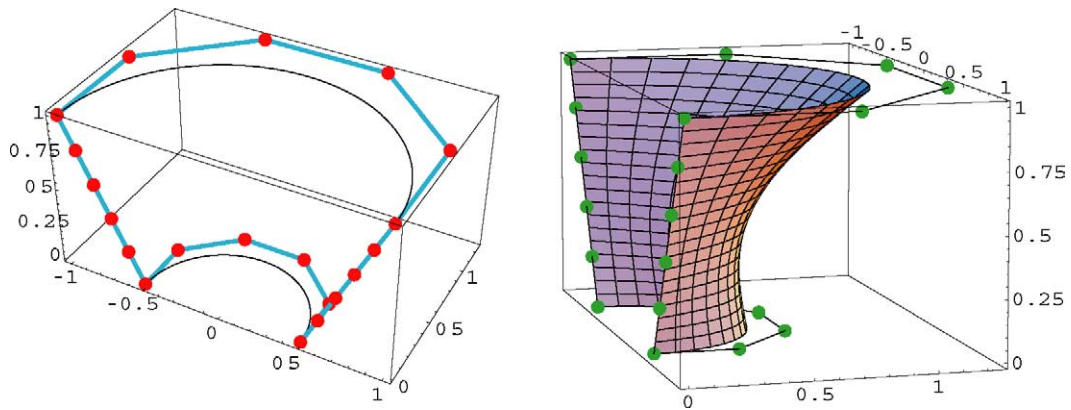


Fig. 2. Left: Boundary curves for the model problem. Right: Biharmonic Bézier surface associated with the boundary conditions of the model problem shown on the left.

the biharmonic equations for high degrees involves the solution of a large linear system, not particularly well conditioned.

4. A comparative study between harmonic and biharmonic Bézier surfaces

In this section we discuss a study we have undertaken to compare between harmonic and biharmonic Bézier surfaces. In particular, we compare the numerical values of the resulting surface area and both harmonic and biharmonic functionals with the corresponding extremals. We have also compared the functionals for harmonic masks as well as the biharmonic surfaces. As a means of checking the surface quality and making qualitative comparisons of the harmonic and biharmonic Bézier surfaces we also compare the corresponding absolute mean curvature distributions for the surfaces.

Before we present our numerical comparisons and qualitative analysis for the surfaces we discuss the extremals of the functionals and the finite difference masks discussed in Section 1 in relation to the harmonic and biharmonic Bézier surfaces discussed in Sections 2 and 3, respectively.

4.1. Extremals of harmonic and biharmonic functionals

4.1.1. Extremals of the harmonic functional

As discussed earlier in Section 1 the Lagrange functional generating the Laplacian operator is given in Eq. (2) which is also known as the Dirichlet functional in the theory of minimal surfaces.

Here we show some results that translate the condition “a control net \mathcal{P} is an extremal of the Dirichlet functional” into a system of linear equations in terms of the control points. Note that here we are not computing the Euler–Lagrange equations of the Dirichlet functional. Instead, we will simply compute the points where the gradient of a real function defined on $\mathbb{R}^{3(n-1)(m-1)}$ vanishes. In other words, what we are studying are the critical points of the function, $\mathcal{P} \rightarrow \mathcal{D}(\vec{\mathbf{x}}^{\mathcal{P}})$, where $\vec{\mathbf{x}}^{\mathcal{P}}$ denotes the Bézier patch associated to the control net \mathcal{P} . The following result for which details can be found in (Monterde, 2004) describes how harmonic Bézier surfaces are related to the corresponding extremals.

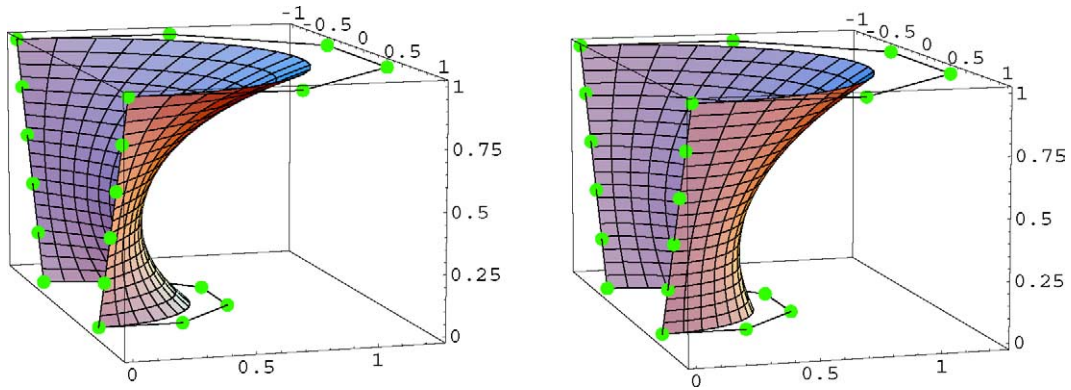


Fig. 3. The associated Bézier surface extremal of the harmonic functional (left) and the biharmonic functional (right) for boundary curves shown in Fig. 2 left.

Proposition 3. A control net, $\mathcal{P} = \{P_{ij}\}_{i,j=0}^{n,m}$, is an extremal of the harmonic functional with prescribed border if and only if

$$0 = \frac{n^2}{(n-1)(m-j)} \sum_{k,\ell=0}^{n-1,m} \frac{\binom{m}{\ell}}{\binom{2m}{j+\ell}} A_{ni}^k \Delta^{10} P_{k\ell} + \frac{m^2}{(m-1)(n-i)} \sum_{k,\ell=0}^{n,m-1} \frac{\binom{n}{k}}{\binom{2n}{i+k}} A_{mj}^\ell \Delta^{01} P_{k\ell}, \quad (15)$$

for any $i \in \{1, \dots, n-1\}$ and $j \in \{1, \dots, m-1\}$ where A_{ni}^k is defined by

$$\frac{ni - nk - i}{(n-i)(2n-1-i-k)} \frac{\binom{n-1}{k}}{\binom{2n-2}{i+k-1}}.$$

Moreover, given a fixed boundary, the extremal always exists and it is unique.

We now apply this result to our model problem with semi circular boundaries where the side boundaries are also taken into account as shown in Fig. 2, left. The associated Bézier surface extremal of the harmonic functional is shown in Fig. 3, left.

4.1.2. Extremals of the biharmonic functional

The Lagrange functional defining the biharmonic Laplacian operator is discussed in Section 1 and is given by the Eq. (3).

The extremals of the biharmonic functional can also easily be computed. Again, as with the harmonic case what we are studying are the critical points of the function

$$\mathcal{P} \rightarrow \mathcal{B}(\bar{\mathbf{x}}^{\mathcal{P}}),$$

where $\bar{\mathbf{x}}^{\mathcal{P}}$ denotes the Bézier patch associated with the control net \mathcal{P} .

Fig. 3, right, shows the Bézier surface extremal of the biharmonic functional. Although the surface is not biharmonic, as can be seen in the figure and from the results we have obtained for the different examples we saw no significant differences between the extremals of biharmonic surfaces and the corresponding biharmonic Bézier surfaces. Detailed discussions on the differences between biharmonic extremals and the corresponding biharmonic Bézier surfaces as well as deduction of the conditions that

such extremals of the biharmonic functional must fulfil in order for them to be biharmonic is beyond the scope of this paper. Nevertheless, as a means of comparison, for the examples discussed below we provide the results of the corresponding Bézier surfaces obtained as the biharmonic extremals.

4.2. Masks for harmonic and biharmonic Bézier surfaces

4.2.1. The harmonic mask

A simple way of constructing Bézier surfaces with prescribed boundary involves generating the inner control points by using the harmonic mask which arises from the discretisation of the Laplacian operator as described in Section 1.

Let us recall that a mask is a linear relation between one inner control point and its eight neighbouring control points. To compute this we need to solve a system of linear equations whose matrix of coefficients form a sparse matrix, i.e., a matrix with just a few non-vanishing entries. For an $n \times m$ Bézier surface, there are $(n - 1) \times (m - 1)$ linear equations and the same number of inner control points. With this setting, the numerical values of the harmonic functionals for the corresponding harmonic Bézier surfaces can be computed.

4.2.2. The biharmonic mask

A discretisation of the biharmonic operator produces a kind of mask of higher order given in equation statement (7). We note that this kind of mask cannot be used to solve the related biharmonic Bézier problem since the prescribed data in our case is simply the boundary curves. The use of the biharmonic mask, on the other hand, requires the knowledge of the boundary curves as well as that of the partial derivatives along the boundary curves, or equivalently, in terms of control points of a Bézier surface, the boundary control points and the control points adjacent to the boundary control points.

4.3. Examples

To present our comparative study here we discuss several examples of biharmonic Bézier surfaces, including the model problem discussed earlier. For each example the results are presented in a tabulated form followed by a short discussion.

4.3.1. Example 1

As a first example we discuss our model problem, where Table 1 summarises the results.

As can be noted we found that the best results for the harmonic functional were obtained for the surface corresponding to the harmonic extremal. Similarly, the best results for the biharmonic functional were obtained for the surface corresponding to the biharmonic extremal.

Table 1
Comparative results for the model problem

Functional	Har. extremal	Har. mask	Bihar. surface	Bihar. extremal
Area	2.57882	2.53203	<u>2.51508</u>	2.51679
Harmonic	<u>2.78117</u>	2.83688	2.95473	2.96027
Biharmonic	27.68557	22.91089	21.37350	<u>20.46343</u>

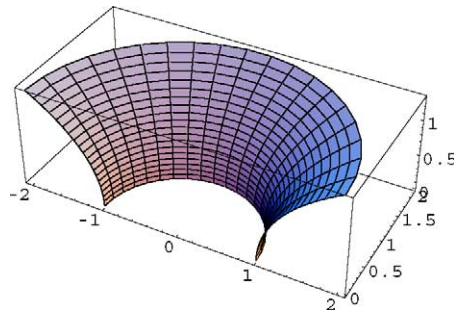


Fig. 4. The catenoid $(\cosh(v) \cos(u), \cosh(u) \sin(u), v)$, a minimal surface, for $u \in [0, \pi]$ and $v \in [0, \operatorname{argcosh}(2)]$. The boundary curves are degree 5 Bézier approximations to the boundary curves of the catenoid.

Table 2
Comparative results for the catenoid, Fig. 4

Functional	Catenoid	Har. extremal	Har. mask	Bihar. surface	Bihar. extremal
Area	7.51007	8.31778	8.00677	<u>7.77847</u>	7.79836
Harmonic	7.51007	<u>9.18563</u>	9.38326	9.82239	9.88235
Biharmonic	10.8828	113.941	96.5717	89.2635	<u>86.1143</u>

4.3.2. Example 2

As a second example we take the catenoid parametrised by

$$(\cosh(v) \cos(u), \cosh(u) \sin(u), v)$$

as shown in Fig. 4, which is a minimal surface for $u \in [0, \pi]$ and $v \in [0, \operatorname{argcosh}(2)]$. The boundary curves in this case are degree 5 Bézier approximations to the boundary curves of the catenoid. Table 2 summarises the corresponding comparative results.

The better approximation to the true area is again the biharmonic surface. Note that the equality between the area and the value of the harmonic functional for the catenoid is a consequence of the fact that for isothermal parametrisations, the area and the harmonic functional agree.

4.3.3. Example 3

As a third example we take an example discussed in (Farin and Hansford, 1999) as shown in Fig. 5. Note that the boundary control points in this case are located on semicircles of radii 4. Table 3 summarises the corresponding comparative results.

In Fig. 6 we show the control nets for the harmonic extremal and biharmonic surface. Here one could observe the regularity of the control net of the biharmonic surface as opposed to the irregular behaviour of the control net of the harmonic extremal.

4.3.4. Example 4

As a fourth and final example we take the four sided figure shown Fig. 7. This particular example is taken from (Monterde, 2003), where the boundary curves are degree 5 Bézier approximations to the semicircles of radii 1. Table 4 summarises the corresponding comparative results.

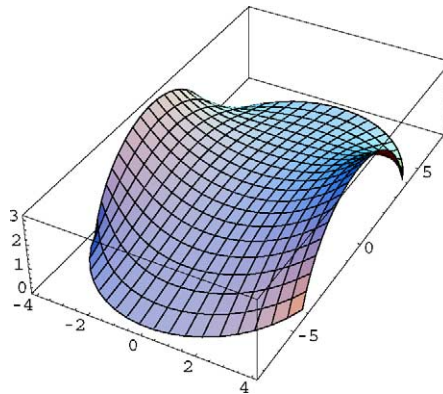


Fig. 5. An example taken from (Farin and Hansford, 1999). Boundary control points are located on semicircles of radii 4.

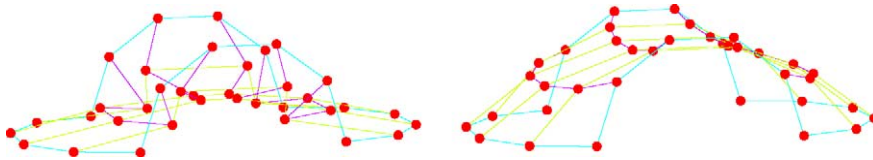


Fig. 6. Control nets of the harmonic extremal (left) and the biharmonic surface (right) for Fig. 5.

Table 3

Comparative results for the example in Fig. 5

Functional	Har. extremal	Har. mask	Bihar. surface	Bihar. extremal
Area	<u>112.38</u>	113.447	118.874	114.345
Harmonic	<u>127.657</u>	129.235	138.235	131.691
Biharmonic	739.017	591.692	696.213	<u>545.73</u>

For the above examples one could note that, in some cases, the method resulting in the smallest surface area is for the biharmonic Bézier surfaces. It is also noteworthy that the results obtained by the methods presented here for the model problem are even better than those obtained by the minimisation of the harmonic or biharmonic functionals. This is indeed true when isothermal conditions are present at the corners, for example the model problem and for the catenoid example. However, when isothermal conditions are absent at the corners, for example as in Fig. 5, the biharmonic Bézier surface fails to be the one with the smaller value for its surface area. For a highly nonisothermal case, for example as in Fig. 7, the difference between the extremal of the harmonic functional and the biharmonic surface is even visible to the naked eye. In this case, the biharmonic surface generated by four curves on a sphere, is very similar to the piece of the sphere limited by the four curves.

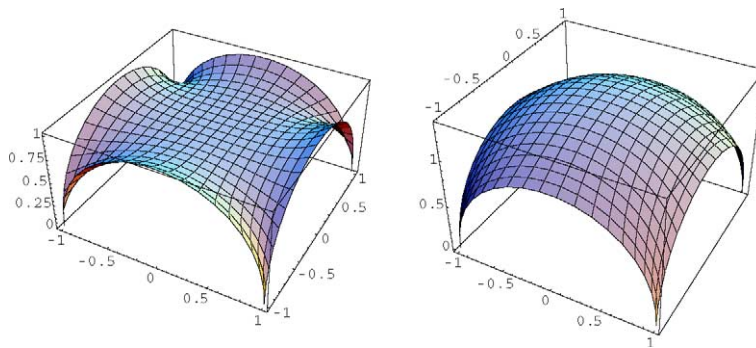


Fig. 7. Another example taken from (Monterde, 2003). Left, the harmonic extremal. Right, the biharmonic surface. The boundary curves are degree 5 Bézier approximations to the semicircles of radius 1.

Table 4
Comparative results for the example in Fig. 7

Functional	Har. extremal	Har. mask	Bihar. surface	Bihar. extremal
Area	4.5887	<u>4.41579</u>	5.00357	5.03371
Harmonic	<u>5.15927</u>	5.4736	6.25076	6.30423
Biharmonic	84.1009	58.1741	51.6785	<u>49.5086</u>

4.4. Qualitative analysis of surfaces

In order to provide an analysis for the quality of the surfaces, here we provide graphical display of curvature variations for the biharmonic Bézier surfaces, the corresponding extremal surfaces (for the harmonic and the biharmonic functional), and the Bézier surface generated by the harmonic mask. In particular, we present plots of absolute mean curvature distributions for our model problem example and that of Example 4. In each case the range of absolute mean curvature plot has been fixed between 0 and 1 in order to enable one to make easy comparisons between the figures.

Fig. 8 shows the plots of the absolute mean curvature distributions for the surfaces constructed using the boundary conditions for our model problem given in Fig. 2, left. The corresponding surfaces, except the one generated by the harmonic mask, are shown in Figs. 2 and 3.

Fig. 9 shows the plots corresponding to Example 4 discussed above for the four generating methods. In all cases, here the mean curvature at the corners goes to infinity due to the non-regularity of the Bézier surface at these points. Here one could note the significant differences between the harmonic and biharmonic cases.

From the above results for the absolute mean curvature plots one can note two things. Firstly for both the harmonic and the biharmonic Bézier surfaces it can be seen that there is no strong variations in curvature within the surface patches indicating that the surfaces are smooth and fair. Secondly the best smoothness in curvature variations can be observed for the case of biharmonic Bézier surface indicating that in terms of fairness and smoothness the biharmonic Bézier is the best amongst all the surfaces. Indeed one would naturally expect this to be the case as the biharmonic surfaces take into account the second variations in the derivative whilst the harmonic surfaces only take the first variation in the derivative into account.

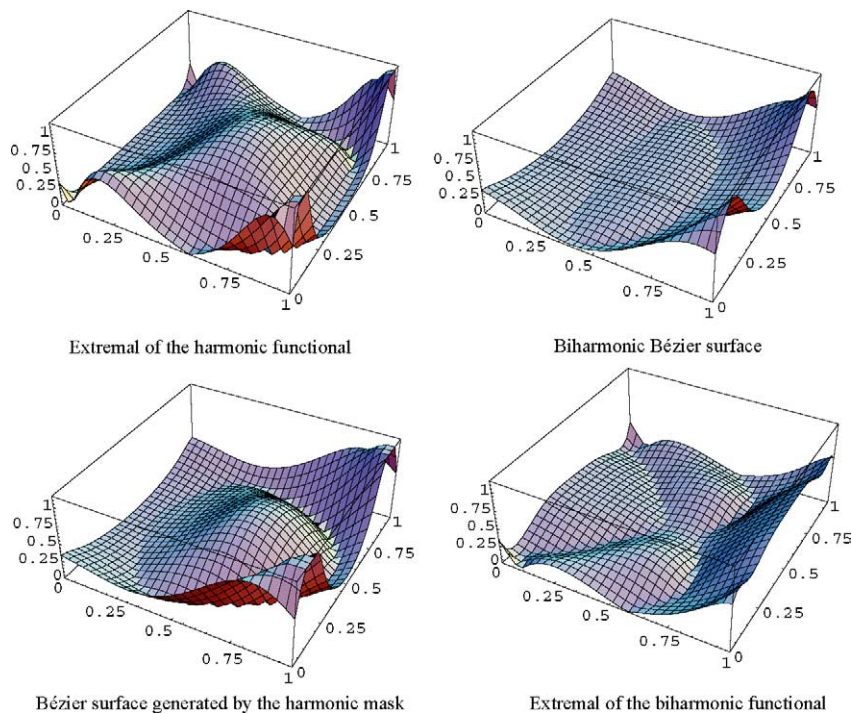


Fig. 8. Plots of the absolute mean curvature for the model problem for the four generating methods.

5. Conclusions

One of the basic problems of computer aided geometric design is the generation of a surface with prescribed boundaries. Depending on the chosen criteria that such a surface must fulfil, different surface generation methods can be found in the literature.

One such criteria is related to the minimisation of the area of the resulting surface. This is based on the highly nonlinear area functional and its Euler–Lagrange equation defining the Laplace–Beltrami operator of the surface. The Laplace–Beltrami operator is an intrinsic operator and is also very difficult to work with. (See (Monterde, 2004, Section 7).) Some of the methods related to the minimisation of the area therefore use the harmonic functional instead and its Euler–Lagrange equation defining the Laplace operator. Unlike the Laplace–Beltrami operator the Laplace operator depends on the parametrisation of the surface, and provides a simpler way of computing good approximations.

For Bézier surfaces, there exist two methods involving the Laplace operator, namely, the use of masks for the discretisation of the Laplace operator and the minimisation of the associated functional, which we refer to as the harmonic functional. A different problem related with the Laplace operator is the determination of harmonic Bézier surfaces. It can be shown that a harmonic Bézier surface is fully determined by the first and last rows of control points.

The main aim of this paper is to show that both problems, i.e., the generation of a surface from its boundary, and the determination of Bézier surfaces verifying a PDE, converge to the biharmonic equation. That is, a biharmonic Bézier surface is fully determined by all of its boundary control points. A very simple and natural model problem has been used throughout the paper to compare the results of

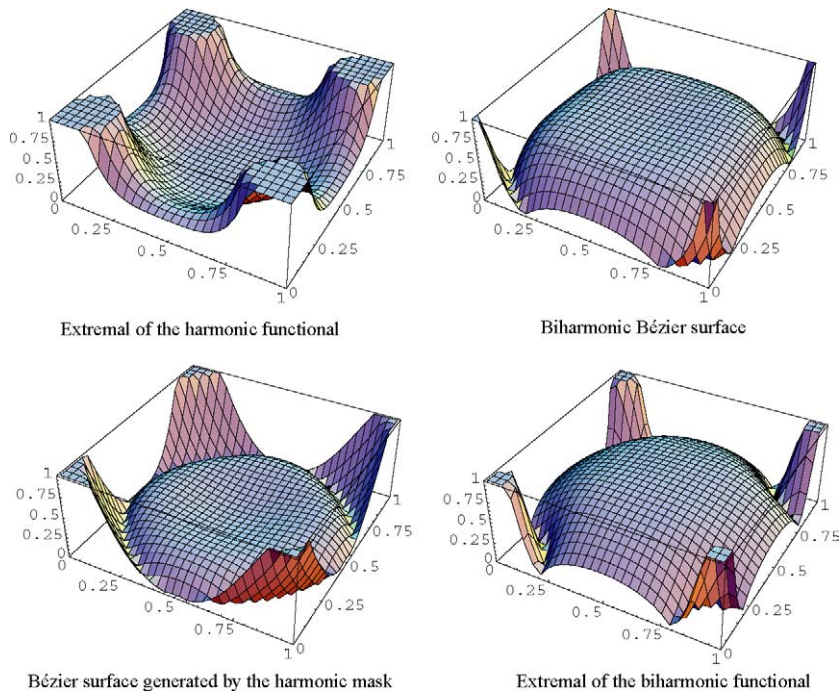


Fig. 9. Plots of the absolute mean curvature for Example 4 and the four generating methods.

the different methods. Furthermore, in Section 4 we have used a collection of other examples involving a variety of different boundary configurations to compare the results of the different methods.

As noted above the biharmonic operator is not an intrinsic operator. Nevertheless, the solutions we have computed here can be considered as approximations to the true solutions of the bilaplace–Beltrami operator. This is due to the fact that when the parametrisation is isothermal, then the Laplace–Beltrami operator is reduced to the Laplace operator, and therefore the bilaplace–Beltrami operator is reduced to the biharmonic operator.

References

- Bloor, M.I.G., Wilson, M.J., 1990. Using partial differential equations to generate freeform surfaces. *Comput. Aided Design* 22, 202–212.
- Farin, G., Hansford, D., 1999. Discrete Coons patches. *Comput. Aided Geom. Design* 16 (7), 691–700.
- Kim, B., Rossignac, J., 2004. Localized bi-Laplacian solver on a triangle mesh and its applications, Georgia Institute of Technology, GVU Technical Report Number: GIT-GVU-04-12.
- Monterde, J., 2004. Bézier surfaces of minimal area: The Dirichlet approach. *Comput. Aided Geom. Design* 21, 117–136.
- Monterde, J., 2003. The Plateau–Bézier problem. In: Wilson, M.J., Martin, R.R. (Eds.), *Mathematics of Surfaces X*. In: *Lecture Notes in Comput. Sci.*, vol. 2768. Springer, Berlin, pp. 262–273.
- Schneider, R., Kobbelt, L., 2001. Geometric fairing of irregular meshes for free-form surface design. *Comput. Aided Geom. Design* 18 (4), 359–379.
- Schneider, R., Kobbelt, L., Seidel, H.-P., 2001. Improved bi-Laplacian mesh fairing. In: Lyche, T., Schumaker, L.L. (Eds.), *Mathematical Methods for Curves and Surfaces*, Oslo, 2000. In: *Innovations In Applied Mathematics Series*. Vanderbilt Univ. Press, pp. 445–454.

Ugail, H., Bloor, M.I.G., Wilson, M.J., 1999. Techniques for interactive design using the pde method. *ACM Trans. Graphics* 18 (2), 195–212.

Ugail, H., 2003. On the spine of a PDE surface. In: Wilson, M.J., Martin, R.R. (Eds.), *Mathematics of Surfaces X*. In: *Lecture Notes in Comput. Sci.*, vol. 2768. Springer, Berlin, pp. 366–376.